

Kinetic model for phase transformation of noncrystalline solids: Application to permanent densification of SiO₂ glass

Daisuke Wakabayashi,^{1,2} Nobumasa Funamori,^{1,2,3} and Tomoko Sato⁴

¹*Institute of Materials Structure Science, High Energy Accelerator Research Organization (KEK), Tsukuba 305-0801, Japan*

²*Department of Materials Structure Science, Graduate University for Advanced Studies, Tsukuba 305-0801, Japan*

³*Department of Earth and Planetary Science, University of Tokyo, Tokyo 113-0033, Japan*

⁴*Department of Earth and Planetary Systems Science, Hiroshima University, Higashi-Hiroshima 739-8526, Japan*



(Received 12 September 2020; accepted 22 March 2021; published 19 April 2021)

The phase transformation of noncrystalline solids is quite different from that of crystalline solids. To gain a better understanding, a kinetic model for pressure-induced phase transformation of noncrystalline solids is constructed by formulating activation- and free-energy distributions. The model is applied to permanent densification of SiO₂ glass, which occurs as a result of a transformation in the network structure. The model is found to be effective in reproducing interesting behavior, including the existence of an infinite number of intermediate states, each of which has a distinct compression curve like a phase, and a halt in the transformation before completion even at sufficiently high temperatures.

DOI: [10.1103/PhysRevB.103.144104](https://doi.org/10.1103/PhysRevB.103.144104)

I. INTRODUCTION

Silica glass is an archetypal oxide glass with a simple chemical formula SiO₂ and a network structure consisting of SiO₄ tetrahedra [1]. It exhibits many characteristic phenomena under high pressure and has received considerable attention in various fields of physical science [2–4]. Permanent densification is particularly interesting. Numerous studies have been conducted since its discovery by Bridgman and Šimon [5] in the 1950s, and the nature of this phenomenon is still explored with state-of-the-art techniques [6]. Nevertheless, the consensus ascribes it to a phase transformation in the network structure, not in the coordination structure [7–14]. The densification can reach up to approximately 20% depending on the applied pressure and temperature [15,16].

It is noteworthy that SiO₂ glasses with densities of 0–20% higher than that of ordinary (i.e., not densified) glass can be synthesized. These glasses exhibit elastic behavior; that is, they have their own compression curves [12,17]. It appears that an infinite number of phases exist. Moreover, it is known that densification proceeds in the pressure range between 4 and 8 GPa even at high temperatures (~900 K), as well as between 9 and 13 GPa at room temperature [12,18]. The phase transformation seems to stop halfway below 8 GPa even at sufficiently high temperatures (i.e., low kinetic barriers).

In the case of crystals, a model based on the kinetics for phase transformation by Cahn [19] and the thermodynamics for grain generation and growth by Turnbull [20] has been widely used [21]. In that model, however, once the phase transformation starts, it does not stop before completion without changes in pressure and/or temperature. Moreover, the intermediate states do not exhibit elastic behavior. Therefore, the model for crystals cannot explain the behavior of permanent densification of SiO₂ glass.

In the case of glasses, Karpov and Grimsditch [22] assumed that the activation energy exhibits a distribution, and they predicted that the phase transformation would evolve linearly with the logarithm of time. On the other hand, Brazhkin and Lyapin [23] assumed that the free energy exhibits a distribution, and they predicted that low- and high-pressure phases coexist as a two-phase mixed intermediate state during the transformation. These predictions were confirmed by experimental studies [24,25]. Advances in experimental techniques have increased the data available on the phase transformation of glasses. However, unlike in the case of crystals, no universal model that can explain the phase transformation has been proposed.

In this study, we propose a kinetic model for pressure-induced structural phase transformation of noncrystalline solids based on a model for crystals in which daughter-phase nuclei are generated and grown within the mother-phase matrix, by formulating activation- and free-energy distributions characteristic of glasses. This is triggered by the recent finding of the coexistence of low- and high-pressure phases during the transformation in glasses [25], in addition to the structural similarity between crystalline and noncrystalline polymorphs [7,12,18,26]. Our model effectively reproduces the interesting behavior of permanent densification of SiO₂ glass, and it provides further insight into the nature of phase transformation of noncrystalline solids.

II. MODEL

A. Energy distribution

The concept of our model is illustrated in Fig. 1. When a phase transformation of glass occurs under applied pressure, two-phase mixed intermediate states are stable in the pressure

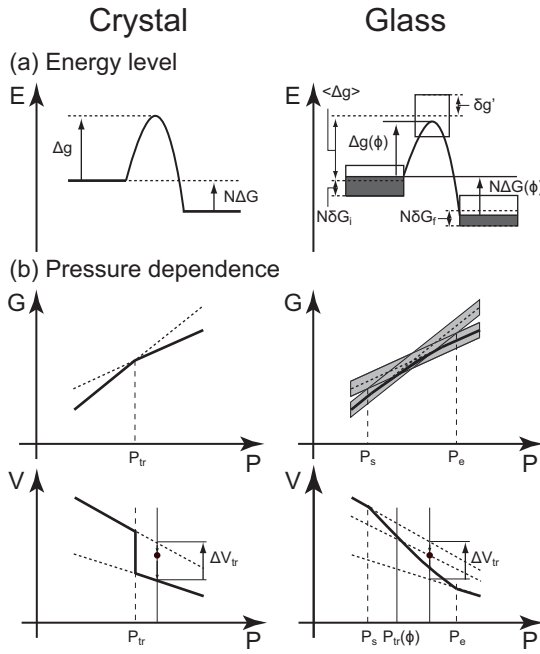


FIG. 1. Schematic illustration of the pressure-induced phase transformation for crystal and glass. (The variables are defined in the main text.)

range from P_s to P_e because of the free-energy distribution. Here, P_s and P_e are the pressures at which the overlap of the energy levels of the two phases starts and ends, respectively. During the transformation, the activation energy Δg and the free-energy difference between the two phases ΔG change with the volume fraction of the daughter phase ϕ , and the balance between them drives or stops the transformation.

For simplicity, the free-energy distribution is assumed to be uniform (rectangular) or Gaussian. In the case of a uniform distribution, Δg is expressed as

$$\Delta g = \langle \Delta g \rangle + \delta g(2\phi - 1). \quad (1)$$

The angular brackets denote the average over ϕ (i.e., the value at $\phi = 0.5$). The width of the activation-energy distribution δg is calculated from the width of the free-energy distribution of the transient state $\delta g'$ and the width of the molar free-energy distribution of the mother phase δG_i via

$$\delta g = \delta g' + N\delta G_i, \quad (2)$$

where N is the number of constituent molecules of the unit associated with the phase transformation. The activation energy and the molar free energy are expressed in units of kJ/unit and kJ/mol in this study, respectively (1 unit is equal to 1 mol for $N = 1$). The subscripts i and f denote the mother and daughter phases, respectively. If it is not necessary to refer to the mother phase, as in the case of ϕ , the subscript f for the daughter phase is omitted for simplicity. ΔG can be expressed in terms of $\Delta V_{tr} \equiv V_i - V_f$ (V is the molar volume) as

$$\Delta G = \int_{P_{tr}}^P \Delta V_{tr} dP', \quad (3)$$

where P is the pressure of the system. P_{tr} is the pressure at which the volume fraction of the daughter phase becomes ϕ

with the passage of thermodynamically sufficient time, that is, the pressure at which $\Delta G = 0$ with $V = (1-\phi)V_i + \phi V_f$. Assuming a uniform energy distribution, P_{tr} satisfies the equation

$$\int_{P_s}^{P_{tr}} \Delta V_{tr} dP' = \phi \int_{P_s}^{P_e} \Delta V_{tr} dP'. \quad (4)$$

Using the defined parameters,

$$\delta G = \delta G_i + \delta G_f \equiv \frac{1}{2} \int_{P_s}^{P_e} \Delta V_{tr} dP', \quad (5)$$

$$\langle \Delta G \rangle \equiv \int_{P_s}^P \Delta V_{tr} dP' - \delta G, \quad (6)$$

Eq. (3) can be simplified as

$$\Delta G = \langle \Delta G \rangle - \delta G(2\phi - 1). \quad (7)$$

In the case of a Gaussian distribution, Eqs. (1) and (7) can be rewritten as

$$\Delta g = \langle \Delta g \rangle + \delta g \operatorname{erf}^{-1}(2\phi - 1), \quad (8)$$

$$\Delta G = \langle \Delta G \rangle - \delta G \operatorname{erf}^{-1}(2\phi - 1). \quad (9)$$

The number of states satisfying $\Delta G = 0$ at $P = P_s$ (or P_e) is $1/e$ of that at $P = \langle P_{tr} \rangle$.

B. Transformation rate

The Avrami equation is widely used in kinetic models for the phase transformation of crystalline materials [19,27]. The Kohlrausch-Williams-Watts function, which is often used in relaxation models for noncrystalline materials [28], has the same form as the Avrami equation. In our model, the volume fraction of the daughter phase ϕ is assumed to follow the Avrami equation,

$$\phi = 1 - \exp(-\phi_{ex}). \quad (10)$$

Here, ϕ_{ex} denotes the extended volume fraction, which is the volume fraction assuming that the daughter-phase grains never stop growing and that new grains keep nucleating at the same rate in transformed domains as well as in untransformed domains [19,27]. When daughter-phase nuclei are generated at a rate \dot{n} and grow spherically at a rate \dot{x} , the volume of the daughter phase v at time τ is expressed as

$$v = \frac{4\pi}{3} \left(\int_{\tau}^t \dot{x} dt' \right)^3. \quad (11)$$

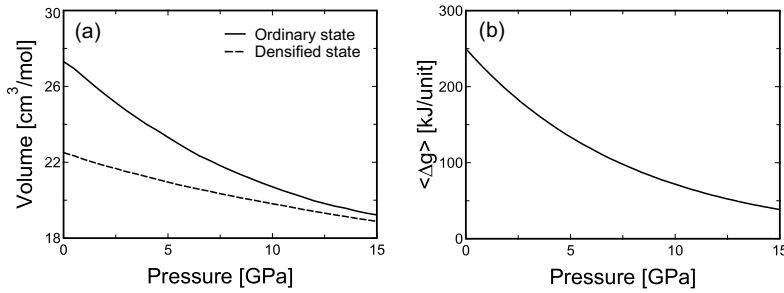
Integrating v with respect to τ , ϕ_{ex} can be expressed as

$$\phi_{ex} = \int_0^t \dot{n} v d\tau. \quad (12)$$

\dot{n} and \dot{x} can be expressed as [20]

$$\dot{n} = aT \exp\{-16\pi\Phi\gamma^3/(3\Delta G_v^2 kT)\} \exp(-\Delta g/RT), \quad (13)$$

$$\dot{x} = bT \exp(-\Delta g/RT)\{1 - \exp(-N\Delta G/RT)\}, \quad (14)$$

FIG. 2. Pressure-dependent parameters for the densification of SiO₂ glass.

where T , γ , k , and R are the temperature of the system, the interfacial energy, the Boltzmann constant, and the gas constant, respectively (a , b , and Φ are constants). In this study, Φ is included in γ , assuming that $\Phi = 1$. ΔG_v is the free-energy difference between the two phases per unit volume, defined as $\Delta G_v \equiv \Delta G/V_f$, which is independent of N . This kinetic model, the evolution of ϕ with t , is applicable to glass, using the Δg and ΔG formulated in the preceding section.

In our model, when the phase transformation proceeds, the total interfacial area between the two phases can be assumed to be unchanged, and thus ϕ satisfies the equation

$$\frac{d\phi}{dt} = A\dot{x}. \quad (15)$$

Here, A is the total interfacial area per unit volume. The value of $\{1 - \exp(-N\Delta G/RT)\}$ in Eq. (14) does not change significantly with time. Thus, by neglecting its time evolution, the solution to Eq. (15) can be obtained from Eqs. (1) and (14):

$$\phi \propto \frac{RT}{2\delta g} \ln t. \quad (16)$$

This is consistent with the model proposed by Karpov and Grimsditch [22], who predicted a linear relationship between the evolution of transformation and the logarithm of time.

III. CALCULATION

A. Discretized expression

In the case of the phase transformation of noncrystalline solids, \dot{n} and \dot{x} are functions of ϕ , and therefore the time evolution is numerically calculated with the following equation obtained by differentiating Eq. (10):

$$\Delta\phi = (1 - \phi)\Delta\phi_{\text{ex}}. \quad (17)$$

Δ represents a small increase only in this section (as different from the usage of Δg and ΔG in other sections). Assuming that daughter-phase nuclei grow spherically, $\Delta\phi_{\text{ex}}$ is expressed as the sum of nucleation and grain growth:

$$\Delta\phi_{\text{ex}} = \frac{4\pi}{3} \dot{n} \Delta t (\dot{x} \Delta t)^3 + A_{\text{ex}} \dot{x} \Delta t. \quad (18)$$

Here, A_{ex} is the extended interfacial area per unit volume, defined in the same way as the extended volume fraction. As in the case of ϕ_{ex} , A_{ex} can be calculated via

$$A_{\text{ex}} = A_{\text{ex}}^* + 4\pi \int_0^t \dot{n} \left(\int_\tau^t \dot{x} dt' \right)^2 d\tau, \quad (19)$$

where A_{ex}^* represents the contribution from the growth of the preexisting daughter phase. $A_{\text{ex}}^* = 0$ if the starting material is a homogeneous mother phase ($\phi = 0$).

B. Contribution of preexisting daughter phase

In the case of intermediately transformed states, the daughter phase already exists at $t = 0$, and A_{ex}^* is not negligible. First, we consider the forward transformation process of intermediately transformed states. When the daughter-phase grains are formed by pretransformation between $t = 0$ and $t = T$ at a nucleation rate \dot{N} and a growth rate \dot{X} , A_{ex}^* is given by

$$A_{\text{ex}}^* = 4\pi \int_0^T \dot{N} R^2 d\tau, \quad (20)$$

where R is the radius of daughter-phase nuclei generated at time τ . R at time t (in the main transformation process) can be obtained by adding the grain growth during the pretransformation and main transformation processes:

$$R = \int_\tau^T \dot{X} dt' + \int_0^t \dot{x} dt'. \quad (21)$$

Next, we consider the reverse transformation process of intermediately transformed states. Assuming that all the daughter-phase grains are spherical with the same radius and distributed without overlapping at $t = 0$ of the reverse transformation process, A_{ex}^* can be calculated via

$$A_{\text{ex}}^* = A_{\text{ex}0}^* \left(1 + \frac{A_{\text{ex}0}^*}{3\phi_0} \int_0^t \dot{x} dt' \right)^2. \quad (22)$$

Here, $A_{\text{ex}0}^*$ and ϕ_0 are the values of A_{ex}^* and ϕ at $t = 0$, respectively.

IV. RESULTS AND DISCUSSION

A. Parameter set

We apply the proposed model to permanent densification of SiO₂ glass. The parameter set proposed in this study is summarized in Fig. 2 and Table I. For V_i and V_f , the pressure dependence shown in Fig. 2(a) was used on the basis of experimental data [12,29]. The $\langle \Delta g \rangle$ at ambient pressure was estimated to be 250 kJ/unit from experimental data for the relaxation process [30]. The $\langle \Delta g \rangle$ at high pressures was assumed to be one order of magnitude smaller than at ambient pressure, on the basis of experimental data for the densification process [15]. It seems reasonable for $\langle \Delta g \rangle$ to decrease

TABLE I. Pressure-independent parameters for the densification of SiO₂ glass^a.

	(i)	(ii)
N	1	5
$\delta g'$	11 kJ/unit	0 kJ/unit
δg		14 kJ/unit
δG_i		2.8 kJ/mol
P_s		3.5 GPa
P_e		10 GPa
γ		0.1 J/m ²
a		$5 \times 10^{33} \text{ m}^{-2} \text{ s}^{-1} \text{ K}^{-1}$
b		$1 \times 10^{-5} \text{ m s}^{-1} \text{ K}^{-1}$

^a $P_s = 10$ GPa and $P_e = 3.5$ GPa in the case of reverse transformation.

with pressure because the difference in volume between low- and high-pressure phases decreases with pressure. Therefore, the pressure dependence of $\langle \Delta g \rangle$ was assumed to be as shown in Fig. 2(b). Assuming that the width of the free-energy distribution is the same for the mother and daughter phases for simplicity, $\delta G_i (= \delta G_f)$ can be calculated using P_s , P_e , and Fig. 2(a) [see Eq. (5)], and δg can be calculated with $\delta g'$, N , and δG_i [see Eq. (2)]. Under these conditions, seven parameters, viz., N , $\delta g'$, P_s , P_e , γ , a , and b , were determined to reproduce the behavior of SiO₂ glass [31].

N should be the number of molecules associated with the phase transformation [20]. In our model, δg controls the time span of the phase transformation, and there is a tradeoff between N and $\delta g'$ as shown in Eq. (2). Therefore, calculations were performed for two extreme cases shown in Fig. 3(a): (i) $N = 1$ and (ii) $\delta g' = 0$. A comparison between the calculation results for cases (i) and (ii) is shown in Fig. 3(b). The results obtained were almost identical; therefore, only case (i) is shown in other figures. For $\delta g' = 0$, $N = 5$ was obtained (Table I). This means that permanent densification can be successfully reproduced only with the free-energy distributions of the mother and daughter phases, by assuming five SiO₂ molecules as the unit of transformation. This seems to corroborate the consensus that permanent densification of SiO₂ glass is ascribable to changes in the network structure consisting of SiO₄ tetrahedra [12,13]. In the case of crystals, N is usually just assumed to be 1 when estimating the activation energy of the phase transformation [21], but N has little effect on the

estimates because the time evolution of the transformation is practically independent of N .

B. Room-temperature behavior

The calculation results for the densification of ordinary glass ($\phi = 0$) at room temperature are shown in Fig. 4(a). As expected on the basis of Eq. (16), ϕ increases almost linearly with the logarithm of time in the middle of the phase transformation ($\phi = 0.2$ – 0.8). The dashed lines represent the calculation results for intermediately densified glass with a densification of 10% ($\phi = 0.5$). The curves are similar to those for ordinary glass at $\phi \geq 0.5$, although further transformation starts earlier, due to the growth of the preexisting daughter phase. In addition, this further transformation is time-shifted (at pressures other than the pressure where the initial state of $\phi = 0.5$ was prepared) because the time evolution of the interface between the mother and daughter phases is pressure-dependent [see Eq. (19)].

The effects of δg are shown in Fig. 4(b). With a larger δg , the phase transformation starts earlier and ends later, indicating that δg has a significant effect on the time span of the transformation. $\delta g = 0$ gives $\delta G = 0$, which corresponds to the phase transformation of crystals [32]. The transformation of crystals proceeds rapidly up to $\phi = 1$ once it starts. In the experiments by Tsiok *et al.* [24], transformation started at a time scale of several tens of seconds, suggesting that the real energy distribution may be close to Gaussian distribution.

The compression behavior of intermediately densified glasses, together with that of ordinary and fully densified glasses, is shown in Fig. 4(c). The transformation of ordinary glass occurs in the pressure range of approximately 9.5–12.5 GPa, which is also seen in Fig. 4(a), and which is consistent with previous experimental data on the permanent densification of SiO₂ glass at room temperature [12]. The transformation of densified glass with $\phi = 0.25$ starts at a slightly lower pressure than ordinary glass, due to the preexisting daughter phase. In the red area, neither forward nor reverse transformation proceeds. This means that intermediately densified glasses exhibit elastic behavior, that is, each of them has a distinct compression curve like a phase at approximately 0–9 GPa. Thus, our model can reproduce the unique feature of permanent densification reported in previous studies [12,17].

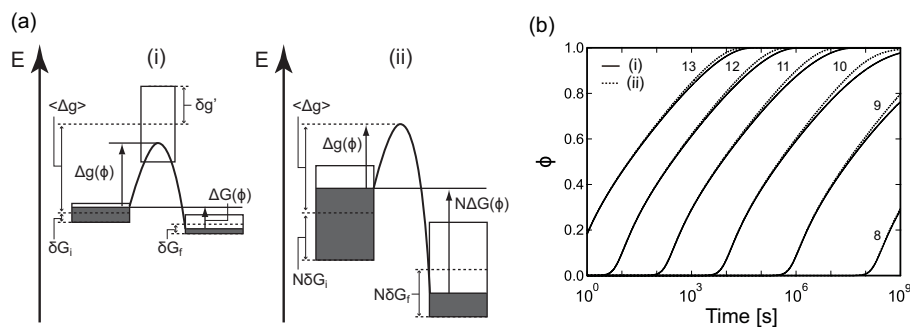


FIG. 3. Comparison between the results for cases (i) $N = 1$ and (ii) $\delta g' = 0$. (a) Schematic illustration of the energy distribution. (b) Time evolution of phase transformation of ordinary glass ($\phi = 0$) at 8–13 GPa. The numbers in the figure represent the pressure in units of GPa.

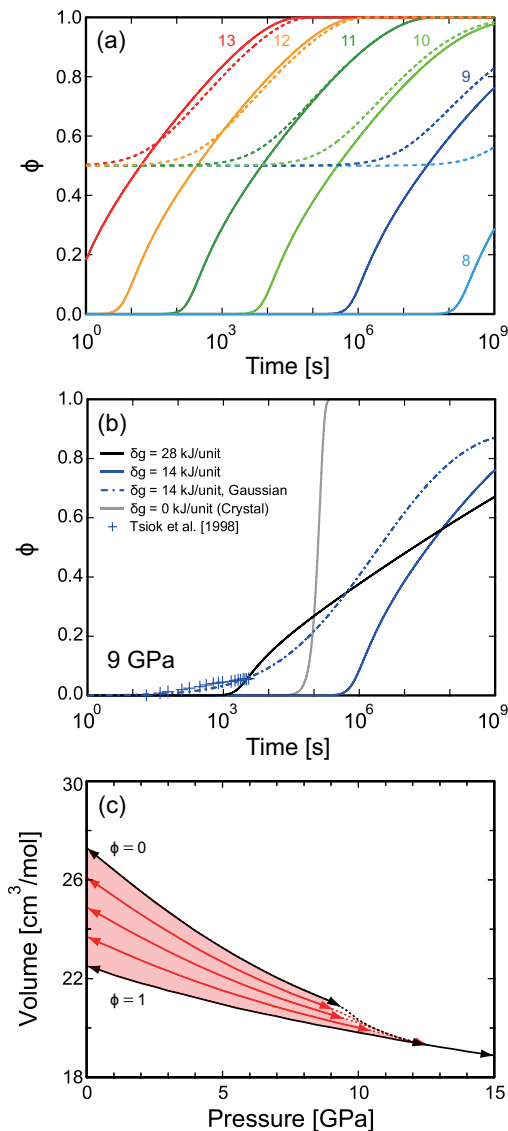


FIG. 4. Phase-transformation kinetics of SiO₂ glass at room temperature. (a) Time evolution of phase transformation of glasses with $\phi = 0$ and 0.5 at 8–13 GPa. The colored numbers represent the pressure in units of GPa. (b) δg dependence of time evolution of phase transformation at 9 GPa. (c) Pressure dependence of molar volume converted from ϕ at $t = 10^5$ s of glasses whose initial densification is $\phi = 0, 0.25, 0.5, 0.75$, and 1. Solid double-headed and dashed right arrows represent the pressure range within which each glass shows reversible and irreversible behaviors, respectively. Calculations for the glasses except for $\phi = 0$ were made assuming that the starting state was densified at 11 GPa and room temperature.

C. High-temperature behavior

The calculation results for the densification of ordinary glass at 900 K are shown in Fig. 5(a). At all pressures, the phase transformation proceeds rapidly once it starts, and the calculation results approach the experimental results. However, in the case of a uniform energy distribution, the low nucleation rate delays the onset of the transformation at low pressures. The nucleation rate may be higher at the beginning, as is the case of a Gaussian distribution. In the case of a

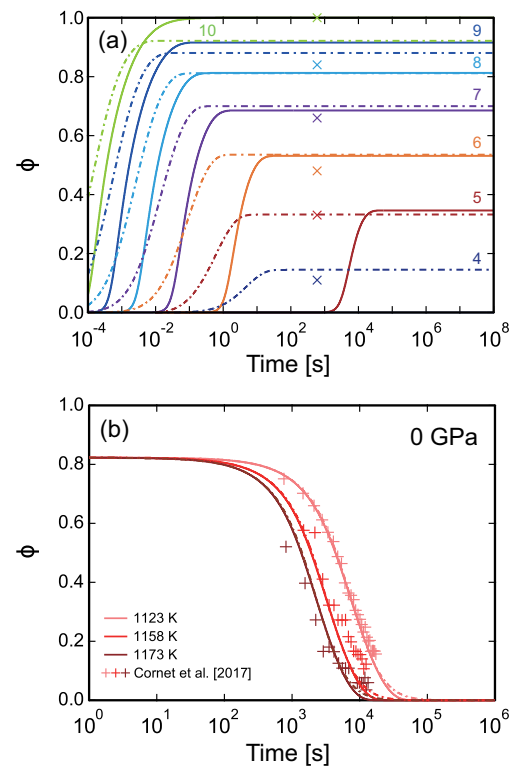


FIG. 5. Phase-transformation kinetics of SiO₂ glass at high temperatures. (a) Time evolution of phase transformation of glass with $\phi = 0$ at 900 K. The colored numbers represent the pressure in units of GPa. Data for densified glasses synthesized with a belt-type high-pressure apparatus (x) are also plotted. (b) Time evolution of reverse transformation of glass with $\phi = 0.82$. Solid and dashed-dotted lines show the calculation results for uniform and Gaussian free-energy distributions, respectively.

Gaussian distribution, however, the overlap of the energy levels of the two phases persists even at $P = P_e = 10$ GPa because of the tail of the Gaussian distribution, thereby preventing the transformation to $\phi = 1$.

The calculation results for the reverse transformation of intermediately densified glass at 0 GPa are shown in Fig. 5(b). The initial densification is 16.5%, corresponding to $\phi = \phi_i = 0.82$ [33]. These calculations can reproduce the experimental data by Cornet *et al.* [30]. The pressure is sufficiently lower than $P_s = 10$ GPa (for reverse transformation) and the temperature is high. Thus, the results for the two types of energy distribution are not different.

V. CONCLUDING REMARKS

The model proposed here successfully reproduces the interesting behavior associated with permanent densification of SiO₂ glass. It should be noted that we have made no assumptions specific to SiO₂ glass in constructing our model. Our model is applicable to other phase transformations in noncrystalline solids. It gives a picture that a two-phase mixed intermediate state emerges during the transformation, and that the transformation proceeds as the domains of each phase grow (or disappear). In addition, the two-phase mixed inter-

mediate states can exhibit elastic behavior as if an infinite number of intermediate phases exist.

For example, we consider the transformations in the coordination structure of SiO₂ and GeO₂ glasses. The transformation of SiO₂ glass between fourfold-coordinated and sixfold-coordinated structures occurs 20–30 GPa on compression and 15–10 GPa on decompression at room temperature [25]; that is, the intermediate states at 25 GPa on compression and 12.5 GPa on decompression are expected to be a two-phase mixture with an average of fivefold coordination [34]. Our model predicts that at 12.5–25 GPa, the intermediate state would exhibit elastic behavior as if a fivefold-coordinated phase existed. GeO₂ glass is known to have much in common with SiO₂ glass, and Guthrie *et al.* [35]

reported a fivefold-coordinated phase. Our model suggests the possibility that they may have observed elastic behavior of a two-phase mixed intermediate state, rather than a fivefold-coordinated phase. We expect that our model will be applied to various noncrystalline solids and contribute to a better understanding of their phase transformations.

ACKNOWLEDGMENTS

The authors thank Y. Murakami and four anonymous referees for their comments. This work was supported in part by JSPS KAKENHI Grants No. JP17K18813 and No. JP20K14584.

-
- [1] W. H. Zachariasen, The atomic arrangement in glass, *J. Am. Chem. Soc.* **54**, 3841 (1932).
- [2] S. Petitgirard, W. J. Malfait, B. Journaux, I. E. Collings, E. S. Jennings, I. Blanchard, I. Kantor, A. Kurmosov, M. Cotte, T. Dane, M. Burghammer, and D. C. Rubie, SiO₂ Glass Density to Lower-Mantle Pressures, *Phys. Rev. Lett.* **119**, 215701 (2017).
- [3] S. J. Tracy, S. J. Turneaure, and T. S. Duffy, *In Situ* X-Ray Diffraction of Shock-Compressed Fused Silica, *Phys. Rev. Lett.* **120**, 135702 (2018).
- [4] S. K. Lee, Y.-H. Kim, Y. S. Yi, P. Chow, Y. Xiao, C. Ji, and G. Shen, Oxygen Quadclusters in SiO₂ Glass above Megabar Pressures up to 160 GPa Revealed by X-Ray Raman Scattering, *Phys. Rev. Lett.* **123**, 235701 (2019).
- [5] P. W. Bridgman and I. Šimon, Effects of very high pressures on glass, *J. Appl. Phys.* **24**, 405 (1953).
- [6] Y. Onodera, S. Kohara, P. S. Salmon, A. Hirata, N. Nishiyama, S. Kitani, A. Zeidler, M. Shiga, A. Masuno, H. Inoue, S. Tahara, A. Polidori, H. E. Fischer, T. Mori, S. Kojima, H. Kawaji, A. I. Kolesnikov, M. B. Stone, M. G. Tucker, M. T. McDonnell, A. C. Hannon, Y. Hiraoka, I. Obayashi, T. Nakamura, J. Akola, Y. Fujii, K. Ohara, T. Taniguchi, and O. Sakata, Structure and properties of densified silica glass: Characterizing the order within disorder, *NPG Asia Mater.* **12**, 85 (2020).
- [7] R. J. Hemley, H. K. Mao, P. M. Bell, and B. O. Mysen, Raman Spectroscopy of SiO₂ Glass at High Pressure, *Phys. Rev. Lett.* **57**, 747 (1986).
- [8] S. Susman, K. J. Volin, D. L. Price, M. Grimsditch, J. P. Rino, R. K. Kalia, P. Vashishta, G. Gwanmesia, Y. Wang, and R. C. Liebermann, Intermediate-range order in permanently densified vitreous SiO₂: A neutron-diffraction and molecular-dynamics study, *Phys. Rev. B* **43**, 1194 (1991).
- [9] J. S. Tse, D. D. Klug, and Y. Le Page, High-pressure densification of amorphous silica, *Phys. Rev. B* **46**, 5933 (1992).
- [10] K. Trachenko and M. T. Dove, Compressibility, kinetics, and phase transition in pressurized amorphous silica, *Phys. Rev. B* **67**, 064107 (2003).
- [11] Y. Inamura, Y. Katayama, W. Utsumi, and K. Funakoshi, Transformations in the Intermediate-Range Structure of SiO₂ Glass under High Pressure and Temperature, *Phys. Rev. Lett.* **93**, 015501 (2004).
- [12] D. Wakabayashi, N. Funamori, T. Sato, and T. Taniguchi, Compression behavior of densified SiO₂ glass, *Phys. Rev. B* **84**, 144103 (2011).
- [13] E. Ryuo, D. Wakabayashi, A. Koura, and F. Shimojo, *Ab initio* simulation of permanent densification in silica glass, *Phys. Rev. B* **96**, 054206 (2017).
- [14] The transformation in the coordination structure takes place at higher pressures than that in the network structure, and higher-coordinated glasses are not recovered to ambient pressure.
- [15] J. D. Mackenzie, High-pressure effects on oxide glasses: I, densification in rigid state, *J. Am. Ceram. Soc.* **46**, 461 (1963).
- [16] J. Arndt and D. Stöfler, Anomalous changes in some properties of silica glass densified at very high pressures, *Phys. Chem. Glasses* **10**, 117 (1969).
- [17] D. Vandembroucq, T. Deschamps, C. Coussa, A. Perriot, E. Barthel, B. Champagnon, and C. Martinet, Density hardening plasticity and mechanical ageing of silica glass under pressure: A Raman spectroscopic study, *J. Phys.: Condens. Matter* **20**, 485221 (2008).
- [18] F. S. El'kin, V. V. Brazhkin, L. G. Khvostantsev, O. B. Tsiok, and A. G. Lyapin, *In situ* study of the mechanism of formation of pressure-densified SiO₂ glasses, *JETP Lett.* **75**, 342 (2002).
- [19] J. W. Cahn, The kinetics of grain boundary nucleated reactions, *Acta Metall.* **4**, 449 (1956).
- [20] D. Turnbull, Phase changes, *Solid State Phys.* **3**, 225 (1956).
- [21] D. C. Rubie, Y. Tsuchida, T. Yagi, W. Utsumi, T. Kikegawa, O. Shimomura, and A. J. Brearley, An in situ X ray diffraction study of the kinetics of the Ni₂SiO₄ olivine-spinel transformation, *J. Geophys. Res.* **95**, 15829 (1990).
- [22] V. G. Karpov and M. Grimsditch, Pressure-induced transformations in glasses, *Phys. Rev. B* **48**, 6941 (1993).
- [23] V. V. Brazhkin and A. G. Lyapin, Two scenarios for phase-transformation in disordered media, *JETP Lett.* **78**, 542 (2003).
- [24] O. B. Tsiok, V. V. Brazhkin, A. G. Lyapin, and L. G. Khvostantsev, Logarithmic Kinetics of the Amorphous-Amorphous Transformations in SiO₂ and GeO₂ Glasses under High Pressure, *Phys. Rev. Lett.* **80**, 999 (1998).
- [25] T. Sato, N. Funamori, D. Wakabayashi, K. Nishida, and T. Kikegawa, Coexistence of two states in optically homogeneous silica glass during the transformation in short-range order, *Phys. Rev. B* **98**, 144111 (2018).
- [26] A. I. Chumakov, G. Monaco, A. Fontana, A. Bosak, R. P. Hermann, D. Bessas, B. Wehinger, W. A. Crichton, M. Krisch, R. Rüffer, G. Baldi, G. Carini Jr., G. Carini, G. D'Angelo, E. Gilioli, G. Tripodo, M. Zanatta, B. Winkler, V. Milman, K. Refson, M. T. Dove, N. Dubrovinskaia, L. Dubrovinsky,

- R. Keding, and Y. Z. Yue, Role of Disorder in the Thermodynamics and Atomic Dynamics of Glasses, *Phys. Rev. Lett.* **112**, 025502 (2014).
- [27] M. Avrami, Kinetics of phase change. II. Transformation-time relations for random distribution of nuclei, *J. Chem. Phys.* **8**, 212 (1940).
- [28] *The Glass Transition: Relaxation Dynamics in Liquids and Disordered Materials*, edited by E. Donth (Springer, Berlin, 2001).
- [29] T. Sato, N. Funamori, and T. Yagi, Helium penetrates into silica glass and reduces its compressibility, *Nat. Commun.* **2**, 345 (2011).
- [30] A. Cornet, V. Martinez, D. de Ligny, B. Champagnon, and C. Martinet, Relaxation processes of densified silica glass, *J. Chem. Phys.* **146**, 094504 (2017).
- [31] It has been reported that densified glasses synthesized under different conditions may have a different structure even with the same density [6,30,36–38]. It has also been reported that the boundary region between mother and daughter phases may have an intermediate structure [25]. Although these points were not taken into account for simplicity, the parameter set well reproduces the behavior associated with permanent densification.
- [32] The onset of the transformation for crystals is significantly delayed when all parameters other than δg and δG are the same as those for glasses. In Fig. 4(b), a and b were adjusted for a crystal in order to hasten the onset of the transformation ($a = 1 \times 10^{58} \text{ m}^{-2} \text{ s}^{-1} \text{ K}^{-1}$, $b = 1 \text{ ms}^{-1} \text{ K}^{-1}$).
- [33] The daughter phase is ordinary glass and φ_0 in Eq. (22) is equal to 0.18. $A^*_{\text{ex}0}$ was determined by fitting our model to the experimental data by Cornet *et al.* [30] ($A^*_{\text{ex}0} = 1.5 \times 10^9 \text{ m}^{-1}$).
- [34] The intermediate state is not a single fivefold-coordinated phase, but it could include a transient fivefold-coordinated structure [13,25,39,40].
- [35] M. Guthrie, C. A. Tulk, C. J. Benmore, J. Xu, J. L. Yarger, D. D. Klug, J. S. Tse, H-k. Mao, and R. J. Hemley, Formation and Structure of a Dense Octahedral Glass, *Phys. Rev. Lett.* **93**, 115502 (2004).
- [36] T. Sato, N. Funamori, and T. Yagi, Differential strain and residual anisotropy in silica glass, *J. Appl. Phys.* **114**, 103509 (2013).
- [37] D. Wakabayashi, N. Funamori, and T. Sato, Enhanced plasticity of silica glass at high pressure, *Phys. Rev. B* **91**, 014106 (2015).
- [38] C. Martinet, A. Kssir-Bodon, T. Deschamps, A. Cornet, S. Le Floch, V. Martinez, and B. Champagnon, Permanently densified SiO₂ glasses: A structural approach, *J. Phys.: Condens. Matter* **27**, 325401 (2015).
- [39] C. A. Angell, P. A. Cheeseman, and S. Tamaddon, Pressure enhancement of ion mobilities in liquid silicates from computer simulation studies to 800 kilobars, *Science* **218**, 885 (1982).
- [40] M. Murakami, S. Kohara, N. Kitamura, J. Akola, H. Inoue, A. Hirata, Y. Hiraoka, Y. Onodera, I. Obayashi, J. Kalikka, N. Hirao, T. Musso, A. S. Foster, Y. Idemoto, O. Sakata, and Y. Ohishi, Ultrahigh-pressure form of SiO₂ glass with dense pyrite-type crystalline homology, *Phys. Rev. B* **99**, 045153 (2019).